Nerve growth factor gene therapy using adeno-associated viral vectors prevents cardiomyopathy in type 1 diabetic mice

Nerve Growth Factor Gene Therapy Using Adeno-Associated Viral Vectors Prevents Cardiomyopathy in Type 1 Diabetic Mice

Marco Meloni,[1] Betty Descamps,[1] Andrea Caporali,[1] Lorena Zentilin,[2] Ilaria Floris,[1] Mauro Giacca,[2] and Costanza Emanueli[1]

Diabetes is a cause of cardiac dysfunction, reduced myocardial perfusion, and ultimately heart failure. Nerve growth factor (NGF) exerts protective effects on the cardiovascular system. This study investigated whether *NGF* gene transfer can prevent diabetic cardiomyopathy in mice. We worked with mice with streptozotocin-induced type 1 diabetes and with nondiabetic control mice. After having established that diabetes reduces cardiac NGF mRNA expression, we tested *NGF* gene therapies with adeno-associated viral vectors (AAVs) for the capacity to protect the diabetic mouse heart. To this aim, after 2 weeks of diabetes, cardiac expression of human *NGF* or *β-Gal* (control) genes was induced by either intramyocardial injection of AAV serotype 2 (AAV2) or systemic delivery of AAV serotype 9 (AAV9). Nondiabetic mice were given AAV2–*β-Gal* or AAV9–*β-Gal*. We found that the diabetic mice receiving *NGF* gene transfer via either AAV2 or AAV9 were spared the progressive deterioration of cardiac function and left ventricular chamber dilatation observed in *β-Gal*–injected diabetic mice. Moreover, they were additionally protected from myocardial microvascular rarefaction, hypoperfusion, increased deposition of interstitial fibrosis, and increased apoptosis of endothelial cells and cardiomyocytes, which afflicted the *β-Gal*–injected diabetic control mice. Our data suggest therapeutic potential of NGF for the prevention of cardiomyopathy in diabetic subjects. ***Diabetes* 61:229–240, 2012**

Diabetes is often associated with a specific cardiomyopathy characterized by alterations in systolic and diastolic function as well as microangiopathy. In addition, the diabetic heart suffers the deposition of interstitial fibrosis, which acts as a barrier to myocardial perfusion. The overall result is the development of heart failure during diabetes (1–3).

The neurotrophin nerve growth factor (NGF) is a secreted protein, which binds to its high-affinity tropomyosin-related kinase-A receptor (TrkA). TrkA is expressed on the plasma membrane of neural and nonneural cells, including cardiomyocytes and endothelial cells (4–6). In fact, NGF, via TrkA, is capable of promoting prosurvival effects in both cardiomyocytes and endothelial cells and promotes angiogenesis (4,5,7). Using a mouse model of myocardial infarction induced by coronary artery ligation, we recently demonstrated that adenovirus-mediated intramyocardial *NGF* gene transfer reduces apoptosis of endothelial cells and cardiomyocytes, improves reparative neovascularization, and supports cardiac perfusion (5).

It has been suggested that diabetes alters cardiac NGF expression (8–10). In particular, Ieda et al. (9) described decreased cardiac NGF level after 16 weeks of streptozotocin-induced diabetes in rats, with associated loss of sensory nerve fibers and sensory neuropathy. These effects were also present in diabetic wild-type mice, but *NGF* transgenic mice were spared from diabetes-induced sensory neuropathy (9). Importantly, cardiac *NGF* gene transfer using a hemagglutinating virus of Japan vector rescued diabetes-induced sensory denervation in diabetic rats (9). Moreover, Kaye et al. (11) found reduced cardiac NGF associated with alterations in sympathetic neuronal function and neuroanatomy in nondiabetic rats and humans with congestive heart failure.

To the best of our knowledge, the possibility that cardiac *NGF* gene transfer could prevent diabetes-induced cardiomyopathy has not previously been evaluated. Therefore, we investigated whether increasing the myocardial level of NGF by using adeno-associated viral (AAV) vectors could spare the diabetic heart from failure.

AAVs are small nonenveloped, single-stranded DNA viruses that can potentially infect all cell types and may integrate in the genome of the host cell, making it possible to achieve a long-term transgene expression. Thus far, several AAV serotypes have been identified (12,13). All serotypes share some sequence homology but can have different tissue tropism and receptor-binding characteristics. AAV serotype 2 (AAV2) has been widely used because it possesses a broad tissue tropism. However, biodistribution studies have shown that AAV2 has low efficiency of cardiac transduction after systemic injection (14). Conversely, AAV serotype 9 (AAV9) has been shown to have a preferable muscular transduction after systemic administration (15), making it ideal for noninvasive therapeutic gene transfer of the heart. In the current study, we compared the effect of cardiac NGF overexpression by two different strategies: local intramyocardial injection of an AAV2 vector and systemic AAV9 delivery. We found that *NGF* gene transfer via either approach was able to protect the diabetic heart.

RESEARCH DESIGN AND METHODS

Production, purification, and characterization of AAV vectors. Infectious recombinant AAV particles were generated in human embryonic kidney 293 cells by a cross-packaging approach (16,17) whereby the vector genome was packaged into AAV capsid serotype 2 (18) or capsid serotype 9 (19,20). Viral stocks were obtained by CsCl2 gradient centrifugation. For AAV–human *NGF*

From the [1]Laboratory of Vascular Pathology and Regeneration, Regenerative Medicine Section, School of Clinical Sciences, University of Bristol, Bristol, U.K.; and the [2]Molecular Medicine Laboratory, International Centre for Genetic Engineering and Biotechnology, University of Trieste, Trieste, Italy.
Corresponding author: Costanza Emanueli, c.emanueli@yahoo.co.uk.
Received 3 June 2011 and accepted 15 October 2011.
DOI: 10.2337/db11-0763
This article contains Supplementary Data online at http://diabetes.diabetesjournals.org/lookup/suppl/doi:10.2337/db11-0763/-/DC1.

(*hNGF*) preparation, the complete coding sequence of hNGF was excised from a pCMV-hNGF plasmid (LGC Promochem, Teddington, U.K.) and subcloned in the shuttle vector pAAV-MCS (Agilent Technologies, Edinburgh, U.K.). The plasmids containing the AAV backbones were obtained from Agilent. AAV2-*hNGF* and AAV9-*hNGF* contain a cytomegalovirus promoter, a β-globin intron, and a human growth hormone polyA signal. AAV–*β-Gal* drives the expression of β-galactosidase from a cytomegalovirus promoter and contains an intron from human growth hormone and a polyA signal derived from SV40.

Animals. In vivo experiments were performed in accordance with the *Guide for the Care and Use of Laboratory Animals* (Institute of Laboratory Animal Resources) and covered by U.K. Home Office licenses. Type 1 diabetes was induced in 8-week-old male CD1 mice (30–33 g body wt; Harlan, Blackthorn, U.K.) by five consecutive daily intraperitoneal injections of streptozotocin (40 mg/kg/day in 0.1 mol/l sodium citrate buffer, pH 4.5; Sigma, Dorset, U.K.) (21). Age- and sex-matched nondiabetic control mice were injected with the streptozotocin buffer. Diabetes was confirmed 14 days after the first streptozotocin injection by measurement of glycosuria using Test strips (Clinistix; Bayer, Basel, Switzerland) and reassessed at the moment the mice were killed. Fasting blood glucose levels were additionally measured at 4, 8, and 12 weeks in AAV9-injected mice by using a blood glucose meter (Accu-Check; Roche Diagnostics, Mannheim, Germany). Survival of mice was monitored for the entire duration of the experiments.

In vivo delivery of AAV vectors. Gene transfer of *hNGF* or *β-Gal* control was performed in diabetic mice 14 days after the first streptozotocin injection. AAV2-*hNGF* or AAV2–*β-Gal* was delivered into the left ventricle wall by four injections (total dose of 1×10^{11} viral particles in 20 μL) (5). AAV9-*hNGF* and AAV9–*β-Gal* were injected in the tail vein (total dose of 1.5×10^{12} viral particles in 100 μL). Age-matched nondiabetic mice were injected with either AAV2–*β-Gal* or AAV9–*β-Gal* and used for reference.

Efficiency of cardiac transduction and biodistribution of AAV vectors. Efficiency of cardiac transduction at 2 and 12 weeks after AAV2–*β-Gal* intramyocardial injection was evaluated by X-Gal staining. Moreover, the presence of AAV2-*hNGF* genome was determined by PCR on total DNA isolated from hearts at 2 weeks post–gene transfer. AAV9-*hNGF*–mediated efficiency and duration of transduction in the left ventricle were evaluated by real-time RT-PCR at 2, 4, 8, and 12 weeks post–gene transfer. hNGF biodistribution was additionally determined at 12 weeks post–gene transfer by real-time RT-PCR in the right ventricle, liver, kidney, spleen, and adductor muscles. hNGF cDNA level was normalized to ribosomal protein L32 cDNA level. PCR primers are shown in Supplementary Table 1. In addition, transgenic NGF protein levels were measured by ELISA (Promega, Southampton, U.K.) in mouse plasma at 2 and 12 weeks after gene transfer with either AAV2 or AAV9 and in protein extracts of left ventricle, right ventricle, liver, kidney, spleen, and adductor muscles taken at 12 weeks from AAV9 injections.

Additional expressional analyses of the myocardium. Murine NGF mRNA levels were evaluated by real-time RT-PCR in the left ventricle of streptozotocin-injected diabetic mice (12 weeks) and nondiabetic controls. PCR primers are shown in Supplementary Table 1, available in the Supplementary Data. Western blot analyses of left ventricle for total and phospho(Ser^{473})–Akt-B, total and phospho(Thr^{32})-Foxo3a, and tubulin (all from Cell Signaling, Danvers, MA) were performed at 12 weeks post–gene transfer.

Measurement of cardiac dimensions and function. A high-resolution echocardiography system (Vevo 770; Visual Sonics, Toronto, Canada) was used in anesthetized (880 mmol/kg i.p. tribromoethanol; Sigma) mice to measure the following parameters before gene transfer (baseline) and at 4, 8, and 12 weeks thereafter: heart rate (bpm), left ventricle ejection fraction (LVEF) (measured as percent), left ventricle fractional shortening (LVFS) (percent), left ventricle chamber volume (microliters), and left ventricle internal diameter (LVID) (millimeters) during both systole and diastole (5). Additionally, peak systolic left ventricle pressure (LVP) (millimeters of Hg), maximal rate of LVP rise (dP/dt_{max}) (millimeters of Hg per second), and minimal rate of LVP fall (dP/dt_{min}) (millimeters of Hg per second) were measured with a miniaturized 1.4F Millar tip catheter (Millar Instruments, Houston, TX) at 12 weeks post–gene transfer (5). Moreover, in mice treated with AAV9 vectors, the early-to-atrial velocity ratio (E-to-A ratio) (index of diastolic function) was measured by echocardiography and pulsed Doppler at the level of the mitral valve (22).

Measurement of cardiac perfusion. Absolute myocardial blood flow (milimeters per minute per gram of tissue) was determined at 12 weeks post–gene transfer using fluorescent microspheres (Invitrogen, Paisley, U.K.) as previously described (5,22). Briefly, anesthetized mice (Tribromoethanol) were intubated, and a polyethylene catheter (PE10) was inserted into the right carotid artery and connected to a syringe pump for collection of reference blood. Then, the chest was opened and microspheres (0.02 μm in diameter) were injected into the left ventricle cavity (200 μl of total volume). Reference blood was collected at a rate of 0.15 mL/min. Mice were killed 2 min later, the heart was removed, and the left ventricle was separated, weighed, cut in small pieces, and digested in 10 mL of 2M ethanolic KOH (Sigma) at 60°C for 48 h. Finally, microspheres were collected and fluorescence intensity was determined by a fluorometer.

Histological analyses. At 12 weeks post–gene transfer, hearts were arrested in diastole and perfusion fixed for paraffin embedding. Capillary and arteriole densities were evaluated in left ventricle transverse sections (20× magnification) after staining with isolectin-B4 (endothelial cell marker, 1:100; Invitrogen) and for α-smooth muscle actin (for marking vascular smooth muscle cells, 1:400; Sigma) (5). Apoptosis was determined by transferase-mediated dUTP nick-end labeling (TUNEL) assay (40× magnification) (in situ cell death detection kit Fluorescein; Roche, Indianapolis, IN) (5). TUNEL-positive apoptotic nuclei of endothelial cells were identified on the basis of cell morphology and vascular localization, while cardiomyocytes were considered apoptotic when TUNEL-positive stained nuclei were inside the cardiomyocyte contour. Fibrosis was evaluated using Picrosirius Red staining and revealed by using a polarized light (20× magnification). For each staining, fifteen left ventricle fields were randomly examined and averaged. Infiltrating hematopoietic cells were evaluated (20× magnification) after CD45 (BD Bioscience) staining developed using 3,3′-diaminobenzidine (Dako) followed by Mayer's hematoxylin to counterstain the nuclei.

Statistical analyses. All data are expressed as means ± SEM. ANOVA was used, followed, when appropriate, by unpaired *t* test. Survival curves were analyzed by log-rank test. Analyses were performed using the SigmaStat 3.1 software. A P value <0.05 was interpreted to denote statistical significance.

RESULTS

Myocardial NGF levels decrease in the diabetic mouse heart. Glycosuria (data not shown) and fasting glycemia (measured only in the AAV9 protocol [Supplementary Table 2]) increased in diabetic mice and were not affected by *hNGF* gene transfer. Relative mRNA expression of murine NGF decreased by 7.1-fold in the left ventricle of mice with 12 weeks of diabetes ($P < 0.01$ vs. age-matched nondiabetic controls [Supplementary Fig. 1]).

Transgene expression after AAV gene transfer. X-Gal staining of whole hearts injected 2 and 12 weeks in advance with AAV2–*β-Gal* confirmed successful transduction (Supplementary Fig. 2*A–D*). Additionally, *hNGF* DNA (Supplementary Fig. 2*E*) and hNGF mRNA (Supplementary Fig. 2*G*) were found in hearts that had received AAV2-*hNGF*. hNGF protein was present in the mouse plasma at 2 and 12 weeks after either AAV2-*hNGF* (Supplementary Fig. 2*F*) or AAV9-*hNGF* (Supplementary Fig. 3*D*). hNGF plasma levels were similar in the two groups at 2 weeks (P = not significant) but higher in AAV9-injected mice at 12 weeks ($P < 0.05$). Supplementary Fig. 3*A* shows the presence of hNGF mRNA in the left ventricle of AAV9-*hNGF*–injected mice at different time points. Supplementary Fig. 3*B* shows the hNGF mRNA tissue biodistribution at 12 weeks from intravenous AAV9-mediated gene transfer. After AAV9-*hNGF*, hNGF mRNA expression was higher in the heart (left and right ventricles), adductor muscles, and liver but present in all examined tissues. hNGF protein expression was found in the left and right ventricles, liver, and adductor muscles (Supplementary Fig. 3*C*).

***NGF* gene transfer prevents left ventricle dysfunction in diabetic mice.** A progressive deterioration of cardiac function was observed in *β-Gal*–injected diabetic mice (Tables 1 and 2). In AAV2–*β-Gal* diabetic mice, LVEF and LVFS gradually decreased over time (Table 1), with a significant reduction at 12 weeks post–gene transfer ($P < 0.05$ vs. nondiabetic mice for both comparisons). In AAV9–*β-Gal* diabetic mice (Table 2), LVEF was already diminished at 8 weeks post–gene transfer. By contrast, AAV-mediated *hNGF* gene transfer preserved both LVEF and LVFS (Tables 1 and 2). Ventricular dilatation was evident in diabetic mice compared with nondiabetic controls at 12 weeks post–gene transfer, whereas diabetes-associated left ventricle chamber dilatation and increase in LVID were preserved by

TABLE 1
Cardiac functional and dimensional parameters measured by echocardiography in mice treated with AAV2 vectors

	Nondiabetes AAV2–*β-Gal*	Diabetes AAV2–*β-Gal*	Diabetes AAV2-*hNGF*
Ejection fraction (%)			
Basal	72.12 ± 1.9	72.61 ± 1.5	71.68 ± 1.8
4 weeks	69.12 ± 4.3	65.76 ± 3.4	66.28 ± 2.1
8 weeks	70.03 ± 3.6	64.95 ± 1.4	70.77 ± 1.9
12 weeks	73.05 ± 3.1	**64.60 ± 1.5***	**73.33 ± 1.5††**
Fractional shortening (%)	38.03 ± 1.5	40.35 ± 0.8	38.49 ± 1.7
Basal			
4 weeks	38.74 ± 2.6	36.72 ± 2.1	37.56 ± 2.2
8 weeks	38.21 ± 2.8	35.68 ± 1.1	40.51 ± 1.6
12 weeks	42.54 ± 2.8	**35.26 ± 1.1***	**42.55 ± 1.3††**
LVID (mm)			
End diastolic			
Basal	4.02 ± 0.1	3.90 ± 0.1	3.92 ± 0.2
4 weeks	3.93 ± 0.1	4.01 ± 0.1	3.99 ± 0.1
8 weeks	3.76 ± 0.2	4.19 ± 0.1	4.10 ± 0.1
12 weeks	4.24 ± 0.3	4.42 ± 0.1	4.08 ± 0.1
End systolic			
Basal	2.51 ± 0.1	2.35 ± 0.1	2.42 ± 0.2
4 weeks	2.40 ± 0.3	2.45 ± 0.1	2.43 ± 0.2
8 weeks	2.39 ± 0.2	**2.71 ± 0.1***	2.42 ± 0.5
12 weeks	2.45 ± 0.2	**2.86 ± 0.1***	**2.34 ± 0.1††**
Chamber volume (μL)			
End diastolic			
Basal	74.08 ± 5.1	71.55 ± 1.9	71.69 ± 7.3
4 weeks	74.38 ± 4.2	77.24 ± 4.4	76.22 ± 4.9
8 weeks	72.59 ± 6.5	79.53 ± 3.2	75.70 ± 3.8
12 weeks	81.34 ± 6.4	89.13 ± 4.9	**74.04 ± 4.4†**
End systolic			
Basal	22.32 ± 2.2	20.11 ± 1.1	21.81 ± 4.1
4 weeks	22.67 ± 4.7	25.34 ± 3.2	23.21 ± 2.5
8 weeks	23.54 ± 4.5	28.61 ± 1.9	23.12 ± 1.8
12 weeks	22.74 ± 4.1	**31.66 ± 2.2***	**19.86 ± 1.5††**
Heart rate (bpm)			
Basal	494.4 ± 10.8	480.3 ± 10.2	480.5 ± 8.9
4 weeks	473.1 ± 10.1	**438.8 ± 9.2***	452.6 ± 7.4
8 weeks	461.2 ± 15.4	**392.2 ± 16.1***	**434.7 ± 8.3†**
12 weeks	478.6 ± 15.2	**387.1 ± 15.4***	**455.3 ± 18.6†**

Data are means ± SEM. Measurement after AAV2-mediated gene transfer of either *hNGF* or *β-Gal*. Boldface indicates statistical differences. *$P < 0.05$ vs. nondiabetic mice injected with AAV2–*β-Gal*. †$P < 0.05$ and ††$P < 0.01$ vs. diabetic mice injected with AAV2–*β-Gal* (n = 8–10 mice/group/time point).

either AAV2-*hNGF* or AAV9-*hNGF* (Tables 1 and 2). Heart rate gradually decreased over the time in diabetic mice but was preserved by NGF overexpression (Tables 1 and 2). Figure 1 shows a decrease in E-to-A ratio, indicative of diastolic dysfunction, already at 4 weeks post–gene transfer in AAV9–*β-Gal*–injected diabetic mice. Importantly, AAV9-*hNGF* improved diastolic function (Fig. 1 and Supplementary Table 3). In addition, NGF overexpression improved LVP, dP/dt_{max}, and dP/dt_{min} in diabetic mice (Fig. 2*A–C* for AAV2- and Fig. 2*D–F* for AAV9-injected mice).

***NGF* gene transfer preserves the microvasculature of the diabetic heart and improves myocardial perfusion.** Diabetes causes microvascular rarefaction in the myocardium (23). Indeed, at 12 weeks of diabetes, hearts injected with either AAV2–*β-Gal* or AAV9–*β-Gal* showed reduced densities of capillaries and small (diameter <50 μm) arterioles (Fig. 3). Conversely, cardiac microvasculature was preserved in diabetic hearts overexpressing NGF (Fig. 3*A–C* for AAV2- and Fig. 3*E* and *F* for AAV9-injected mice). The preserved microvessel density was associated with improved cardiac perfusion after *hNGF* gene transfer. In fact, at 12 weeks of diabetes the *β-Gal*–expressing hearts showed a significant reduction of blood flow in comparison with that shown without diabetes. By contrast, both AAV2-*hNGF* and AAV9-*hNGF* improved cardiac perfusion to values similar to those observed in nondiabetic controls (Fig. 3*D* and *G*).

Diabetes is associated with increased apoptosis in the heart (24). Accordingly, left ventricle sections at 12 weeks after diabetes induction and either AAV2–*β-Gal* or AAV9–*β-Gal* showed an increased number of TUNEL-positive apoptotic endothelial cells and cardiomyocytes compared with that shown in nondiabetic controls (Fig. 4*A–F*). By contrast, AAV2-*hNGF* and AAV9-*hNGF* reduced apoptosis of both cardiovascular cell types (Fig. 4*A–C* and *E* for AAV2-treated mice and Fig. 4*D* and *F* for AAV9-treated mice), providing evidence that sustained cardiac NGF expression improves cardiac cell survival under diabetic conditions.

***NGF* gene transfer promotes the activation of the Akt/Foxo3a pathway in the diabetic heart.** The transcription factor Foxo3a triggers apoptosis and negatively regulates

TABLE 2
Cardiac functional and dimensional parameters measured by echocardiography in mice treated with AAV9 vectors

	Nondiabetes AAV9–*β-Gal*	Diabetes AAV9–*β-Gal*	Diabetes AAV9-*hNGF*
Ejection fraction (%)			
Basal	73.90 ± 0.9	72.22 ± 2.2	72.50 ± 0.9
4 weeks	75.12 ± 1.3	72.64 ± 1.1	74.30 ± 0.8
8 weeks	72.87 ± 2.2	**63.83 ± 2.6***	67.93 ± 1.1
12 weeks	72.86 ± 1.6	**63.03 ± 1.7***	**69.44 ± 1.2†**
Fractional shortening (%)			
Basal	41.67 ± 1.1	41.62 ± 2.0	39.99 ± 1.3
4 weeks	40.22 ± 1.5	37.90 ± 1.4	37.46 ± 1.3
8 weeks	38.00 ± 2.6	39.28 ± 2.1	37.41 ± 1.0
12 weeks	41.85 ± 1.5	**34.19 ± 1.2***	**38.48 ± 1.0†**
LVID (mm)			
End diastolic			
Basal	4.01 ± 0.1	4.10 ± 0.1	4.09 ± 0.1
4 weeks	4.30 ± 0.1	4.15 ± 0.1	4.13 ± 0.1
8 weeks	4.09 ± 0.2	4.12 ± 0.2	4.04 ± 0.1
12 weeks	3.96 ± 0.1	**4.49 ± 0.1***	**4.02 ± 0.1†**
End systolic			
Basal	2.38 ± 0.1	2.42 ± 0.1	2.39 ± 0.1
4 weeks	2.67 ± 0.2	2.84 ± 0.1	2.69 ± 0.1
8 weeks	2.53 ± 0.2	2.80 ± 0.1	2.48 ± 0.1
12 weeks	2.32 ± 0.1	**2.89 ± 0.10***	2.54 ± 0.1
Chamber volume (μL)			
End diastolic			
Basal	73.20 ± 2.1	74.65 ± 2.9	74.72 ± 4.3
4 weeks	66.95 ± 1.2	72.59 ± 4.0	68.14 ± 2.2
8 weeks	65.75 ± 2.7	76.48 ± 6.4	64.87 ± 3.7
12 weeks	66.31 ± 4.6	**87.96 ± 5.3****	**72.27 ± 4.6†**
End systolic			
Basal	22.36 ± 4.8	23.63 ± 2.4	23.13 ± 2.5
4 weeks	23.19 ± 3.1	27.21 ± 0.9	25.25 ± 0.8
8 weeks	24.71 ± 3.1	28.35 ± 3.3	22.44 ± 1.9
12 weeks	19.85 ± 2.3	**32.66 ± 2.7***	**24.13 ± 2.5†**
Heart rate (bpm)			
Basal	501.1 ± 40.1	475.0 ± 19.7	490.7 ± 23.3
4 weeks	500.1 ± 23.3	**442.6 ± 10.4***	467.8 ± 10.4
8 weeks	489.1 ± 30.8	**409.2 ± 20.1***	459.4 ± 12.2
12 weeks	490.5 ± 6.7	**397.2 ± 11.9****	**459.6 ± 11.9†**

Data are means ± SEM. Measurement after AAV9-mediated gene transfer of either *hNGF* or *β-Gal*. Boldface indicates statistical differences. *$P < 0.05$ and **$P < 0.01$ vs. nondiabetic mice injected with AAV9–*β-Gal*. †$P < 0.05$ vs. diabetic mice injected with AAV9–*β-Gal* (n = 10–12 mice/group/time point).

angiogenesis (4,25). It acts downstream of Akt signaling, and Akt-dependent phosphorylation of Foxo3a leads to its inactivation and degradation, thus promoting cell survival (4,26) and angiogenesis (25). We have previously shown that NGF activates the Akt/Foxo3a pathway in cultured cardiomyocytes and in the mouse infarcted heart. We additionally reported that Akt/Foxo3a signaling plays a functional role in NGF-induced cardiomyocyte survival and myocardial angiogenesis (4,5). Moreover, the Akt/Foxo signaling is known to be altered in the diabetic heart (27). As shown in Fig. 6, phospho-Akt (active form) and phospho-Foxo3a (inactive form) were significantly reduced at 12 weeks of diabetes in mice injected with *β-Gal*. Importantly, *NGF* gene transfer normalized the phosphorylated-to-total ratio of both Akt and Foxo3a in the diabetic hearts (Fig. 5*A*–*F*). These data suggest that the Akt/Foxo3a pathway may be involved in the regulation of the antiapoptotic and proangiogenic effects of NGF in the diabetic heart.

***NGF* gene transfer reduces fibrosis in the diabetic heart.** Cardiac interstitial fibrosis was significantly increased in the heart of diabetic control mice—an effect that was prevented by NGF overexpression (Fig. 6*A*–*C*). These data together with the improved perfusion in the *hNGF*-treated heart, decreased apoptosis of endothelial cells, and preserved cardiac microvasculature support the idea that *NGF* gene transfer is able to preserve the functionality of small vessels in the diabetic heart. Of note, no gross evidence of interstitial inflammation was observed in any of the investigated groups (Supplementary Fig. 4).

Effect of diabetes and *NGF* gene transfer on survival of mice. In the current study, survival of mice monitored for 12 weeks showed a substantial increased mortality of both AAV2– and AAV9–*β-Gal*-injected diabetic mice compared with that in AAV2– and AAV9–*β-Gal*-injected nondiabetic mice (Supplementary Fig. 5*A* and *B*). AAV2-*hNGF* did not reduce diabetes-associated mortality. By contrast, diabetic mice given AAV9-*hNGF* did not show higher mortality than nondiabetic controls. Although hallmarks of diabetic cardiomyopathy have been observed during the progression of diabetes, we cannot exclude that noncardiac events, including kidney failure and stroke, may

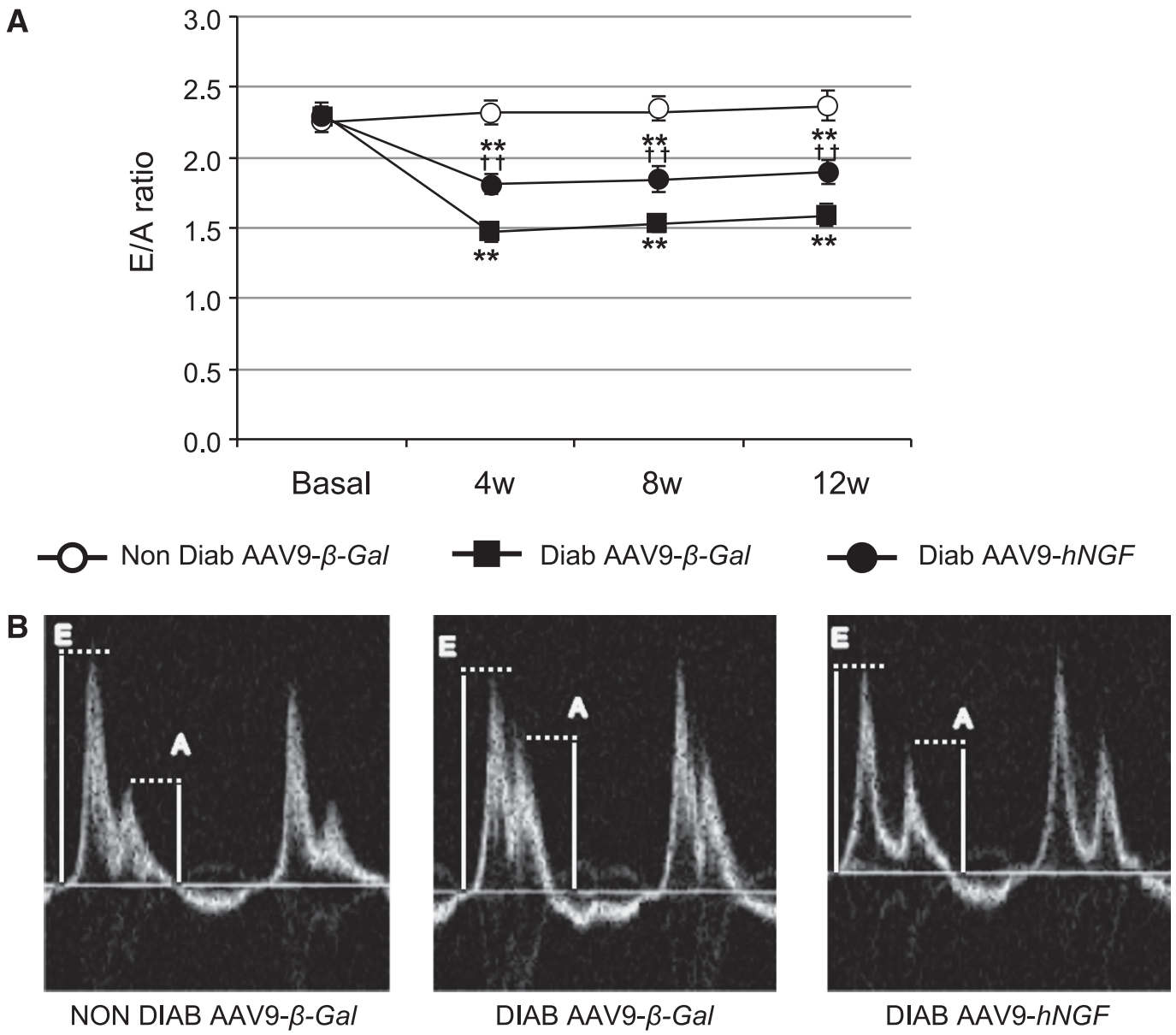

FIG. 1. Effect of AAV9-*hNGF* on diastolic dysfunction after diabetes (Diab). *A*: Graph shows the net reduction of E-to-A ratio (E/A ratio) progressively induced by diabetes in mice injected with AAV9–*β*−*Gal*. This effect was reduced by AAV9-*hNGF*. ○, nondiabetes with AAV9–*β-Gal*; ■, diabetes with AAV9–*β-Gal*; ●, diabetes with AAV9-*hNGF*. *B*: Representative mitral flow patterns from pulsed Doppler at 12 weeks (w) after diabetes induction. Data are expressed as means ± SEM. **$P < 0.01$ vs. nondiabetes with AAV9–*β-Gal*. ††$P < 0.01$ vs. diabetes with AAV9–*β-Gal* (n = 10 mice/group/time point).

have contributed to mortality in the diabetes groups. This would be in line with the improved survival after AAV9-*hNGF*, which determines a wider hNGF biodistribution (Supplementary Figs. 2*G* and 3*B*) and higher circulating hNGF level (Supplementary Figs. 2*F* and 3*D*) in comparison with AAV2-*hNGF*.

DISCUSSION

Diabetes and its several complications are a major public health problem (28). Accumulating evidence from epidemiological data and animal and clinical studies shows that the risk of heart failure is considerably increased by diabetes, and diabetes has been recognized as one of the major risk factors for the development of heart failure (28,29). Nonetheless, the pathophysiology of diabetic cardiomyopathy remains uncertain and novel therapeutic strategies for its prevention and rescue are needed. Several experimental mouse models of type 1 and type 2 diabetes are available, and some, including mice with streptozotocin-induced type 1 diabetes and type 2 diabetic *db/db* mice, have already been shown to develop cardiomyopathy (22,30,31).

Here, we report that AAV-mediated cardiac NGF overexpression inhibits the development of cardiomyopathy in mice with streptozotocin-induced type 1 diabetes. NGF, which was discovered in the nervous system and initially considered with respect to its neural functions (32), was later shown to exert prosurvival actions in the cardiovascular system and to promote angiogenesis, including in the infarcted heart (4,5). Cardiac NGF expression is altered during various pathological conditions. For example, NGF protein levels increase in the peri-infarct area of human

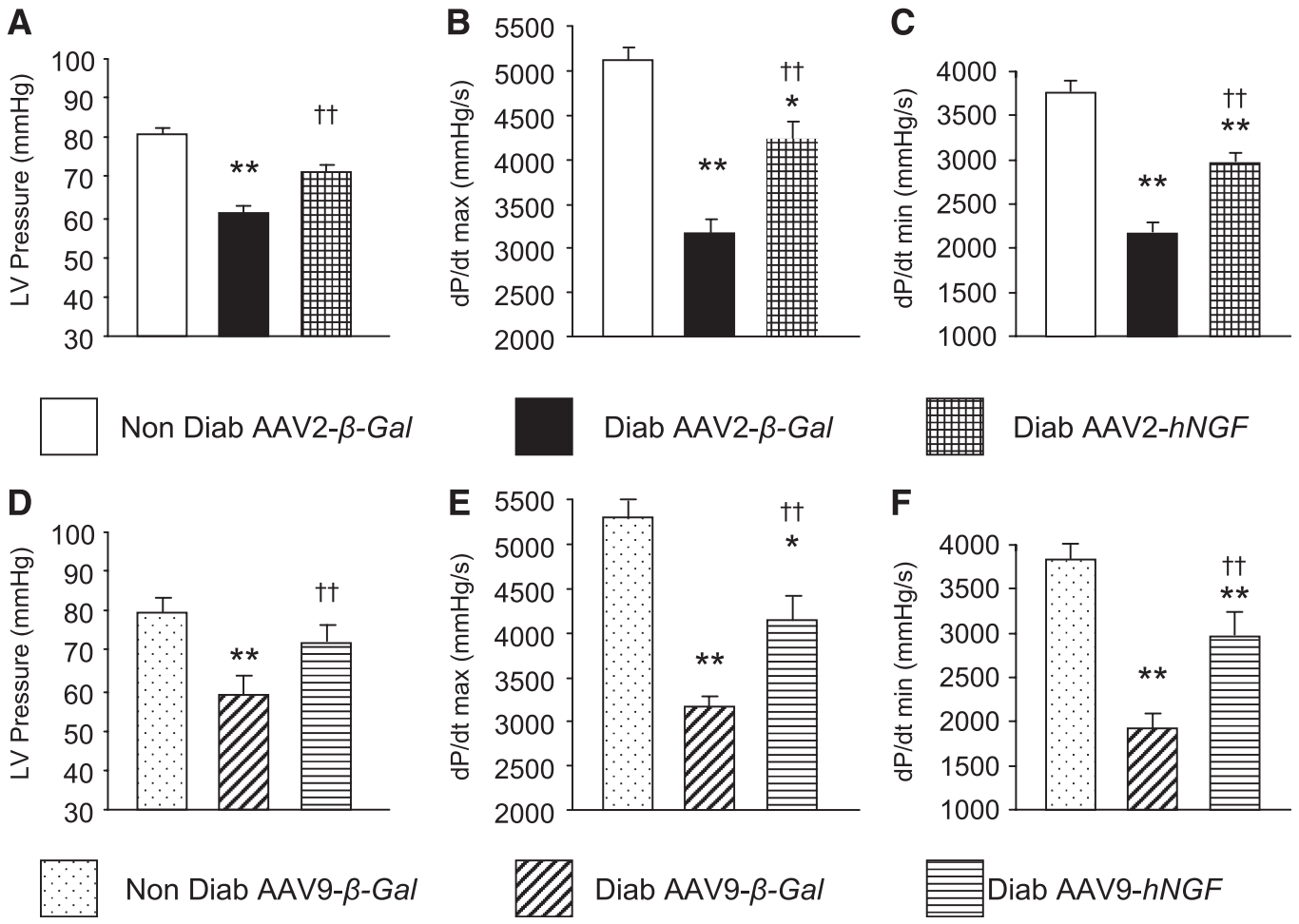

FIG. 2. Impact of AAV2-*hNGF* and AAV9-*hNGF* on left ventricle (LV) function in diabetes (Diab). Analyses by Millar tip catheter at 12 weeks post–gene therapy show left ventricle pressure (*A*), dP/dt_{max} (*B*), and dP/dt_{min} (*C*) in AAV2-injected mice. Bar graphs show left ventricle pressure (*D*), dP/dt_{max} (*E*), and dP/dt_{min} (*F*) in AAV9-treated mice. Data are expressed as means ± SEM. The * symbol indicates statistical differences versus either nondiabetes with AAV2-*β-Gal* or nondiabetes with AAV9-*β-Gal*, while the † symbol indicates differences versus diabetes with either AAV2 or AAV9-*β-gal*. **P* < 0.05 and ***P* < 0.01 vs. either nondiabetes with AAV9–*β-Gal* or nondiabetes with AAV2-*β-Gal*; †*P* < 0.05 and ††*P* < 0.01 vs. either diabetes with AAV9–*β-Gal* or diabetes with AAV2-*β-Gal* (*n* = 8 mice for nondiabetes with AAV2–*β-Gal* [□], *n* = 10 mice for diabetes with AAV2–*β-Gal* [■], diabetes with AAV2-*hNGF* [⊞], and nondiabetes with AAV9–*β-Gal* [⊡]; *n* = 12 mice for diabetes with AAV9–*β-Gal* [▨] and diabetes with AAV9-*hNGF* [▤]).

and mouse hearts early after coronary occlusion (5,33). By contrast, myocardial levels of NGF were reported to be decreased in the setting of diabetes (8,9)—a finding that we have confirmed in the current study. Moreover, the reduction in cardiac NGF was shown to be a major contribution to cardiac diabetic neuropathy, which could be reverted by *NGF* overexpression (9).

The aim of this study was to evaluate the effect of NGF gene transfer on diabetes-induced cardiac dysfunction and microvascular rarefaction. Since diabetes is a chronic disease and the levels of cardiac NGF decrease progressively in the diabetic heart (10), to sustain NGF expression we chose an AAV-based gene transfer approach. In fact, AAVs have the ability to transduce nondividing cells (including cardiomyocytes) in vivo and to achieve a sustained transgene expression. AAV serotypes have minor differences in their capsids, which determine their tropism (12,13). The discrepancies in tissue tropism among the different serotypes are partly due to different mechanisms of uptake into target cells but also to postentry mechanisms involving endosome trafficking, nuclear uptake, and efficiency of viral capsid uncoating (34,35). For example, AAV2 has a broad tropism and infects a wide range of tissues with good efficiency, while AAV9 displays the impressive feature of being able to pass through the endothelial cell barrier of blood vessels when injected systemically, showing substantial levels of transduction in the heart muscle (15). In the current study, we first provided evidence of the beneficial effects of cardiac-specific overexpression of NGF after local intramyocardial injection by using an AAV2. Then, since this method requires an invasive surgery and is therefore not optimal as a potential therapy in cardiac patients or for the welfare of research animals, we additionally tested the cardiac responses to intravenous delivery of AAV9-*hNGF*.

Left ventricle dysfunction is a common feature of the diabetic heart. Throughout the development of diabetes, the contractile capacity of the heart progressively reduces and the heart shows signs of diastolic and systolic alterations. Left ventricle diastolic dysfunction is considered one of the earliest hallmarks occurring in the setting of diabetic cardiomyopathy, and it starts before the onset of systolic dysfunction (36,37). In the current study, cardiac function was measured by echocardiography and pulsed

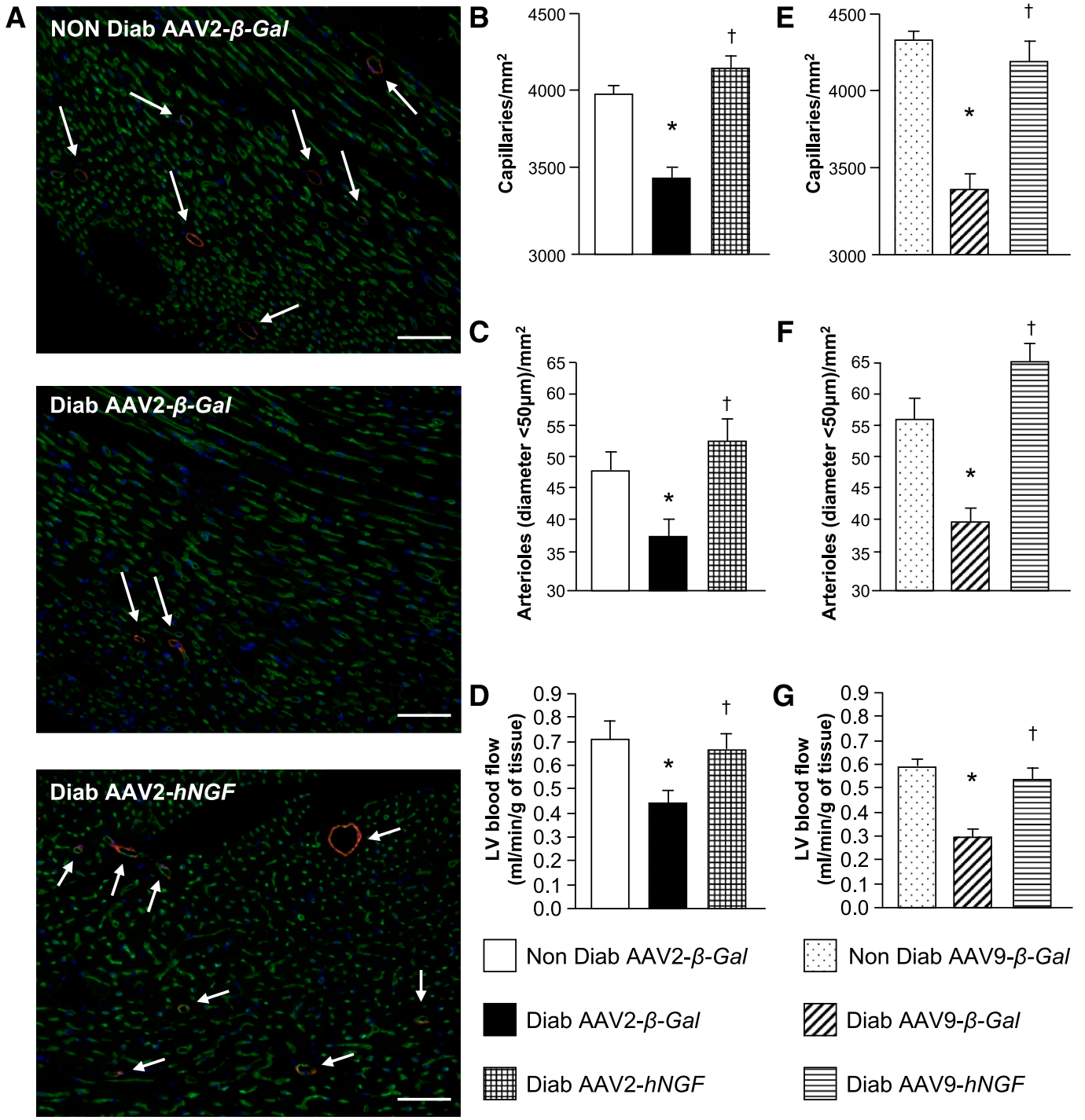

FIG. 3. Impact of AAV-mediated *NGF* gene therapy on cardiac microvasculature and perfusion after diabetes (Diab). *A*: Representative micrographs showing capillaries (stained by isolectin-B4 [green fluorescence]) and arterioles (stained by both isolectin-B4 and α-smooth muscle actin [red and indicated with arrows]) in the left ventricle of AAV2-treated mice. Nuclei are depicted in blue (Dapi). Scale bars: 50 μm. 20× magnification. Bar graphs show the densities of capillaries (*B*) and arterioles (*C*) in AAV2-treated mice. *D*: Bar graph shows the absolute left ventricle myocardial blood flow analyzed by fluorescent microspheres in AAV2-injected mice. Bar graphs show capillary density (*E*), arteriole density (*F*), and left ventricle blood flow (*G*) in AAV9-injected mice. Data are expressed as means ± SEM. *$P < 0.05$ vs. nondiabetes with AAV2–*β-Gal* or nondiabetes with AAV9–*β-Gal*; †$P < 0.05$ vs. diabetes with AAV2–*β-Gal* or diabetes with AAV9–*β-Gal*. (For histological analyses, $n = 5$ mice for each nondiabetes group and $n = 6$ mice for all other groups; $n = 8$ mice/group for blood flow measurement). □, nondiabetes with AAV2–*β-Gal*; ■, diabetes with AAV2–*β-Gal*; ⊞, diabetes with AAV2-*hNGF*; ⊡, nondiabetes with AAV9–*β-Gal*; ▨, diabetes with AAV9–*β-Gal*; ▤, diabetes with AAV9-*hNGF*. (A high-quality digital representation of this figure is available in the online issue.)

Doppler analyses before diabetes induction and then every 4 weeks. Moreover, at the end of the experiment left ventricle function was additionally measured by left ventricle catheterization. In our diabetic mice, echocardiography and pulsed Doppler analyses showed the presence of diastolic dysfunction at early stages of diabetes, which confirms our previous findings (22,30). In fact, *β-Gal*–injected mice exhibited a pronounced decrease in the E-to-A ratio (starting at 4 weeks of diabetes) and of left ventricle dP/dt_{min} (which was assessed as a terminal procedure 12 weeks after

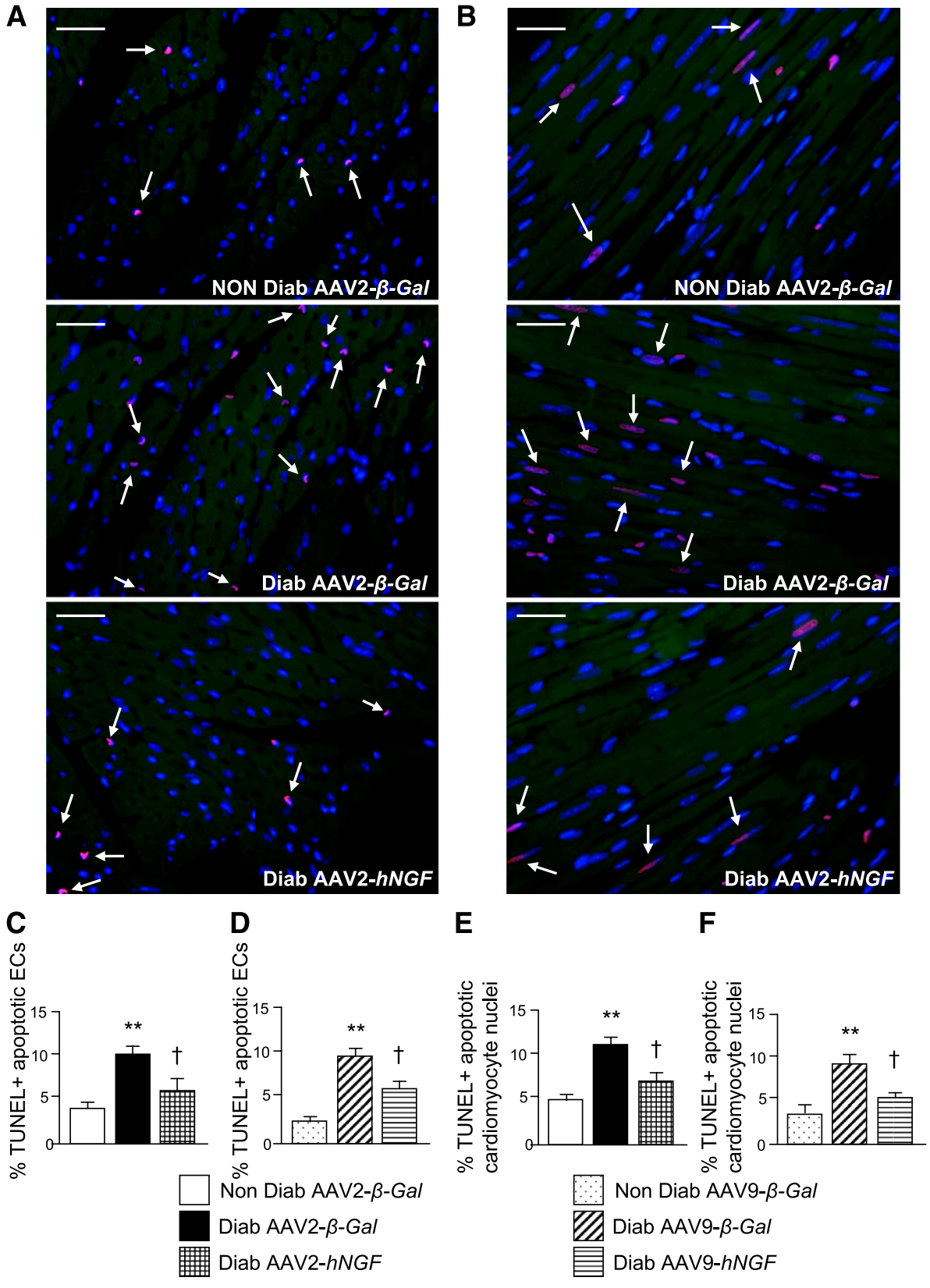

FIG. 4. ***NGF*** **gene therapy reduces apoptosis of endothelial cells (ECs) and cardiomyocytes in the diabetic heart. Representative microphotographs showing TUNEL-positive apoptotic nuclei (in purple and indicated by arrows) of endothelial cells (*A*) and of cardiomyocytes (*B*) in AAV2-injected mice. Nuclei are stained in blue (Dapi). Scale bars: 20 μm. (40× magnification). Bar graphs show the percentage of TUNEL-positive apoptotic endothelial cells (AAV2-treated mice [*C*] and AAV9-injected mice [*D*]) and cardiomyocytes (AAV2-injected mice [*E*] and AAV9-injected mice [*F*]) in the left ventricle 12 weeks after diabetes induction. Data are expressed as means ± SEM. *****P*** **< 0.01 vs. nondiabetes with AAV2–*β-Gal*** **or nondiabetes with AAV9–*β-Gal*; †*P* < 0.05 vs. diabetes with AAV2–*β-Gal*** **or diabetes with AAV9–*β-Gal*** **(*n* = 5 mice for each nondiabetes group and *n* = 6 mice for all other groups). □, nondiabetes with AAV2–*β-Gal*; ■, diabetes with AAV2–*β-Gal*; ⊞, diabetes with AAV2-*hNGF*; ⊡, nondiabetes with AAV9–*β-Gal*; ▨, diabetes with AAV9–*β-Gal*; ▤, diabetes with AAV9-*hNGF*. (A high-quality digital representation of this figure is available in the online issue.)**

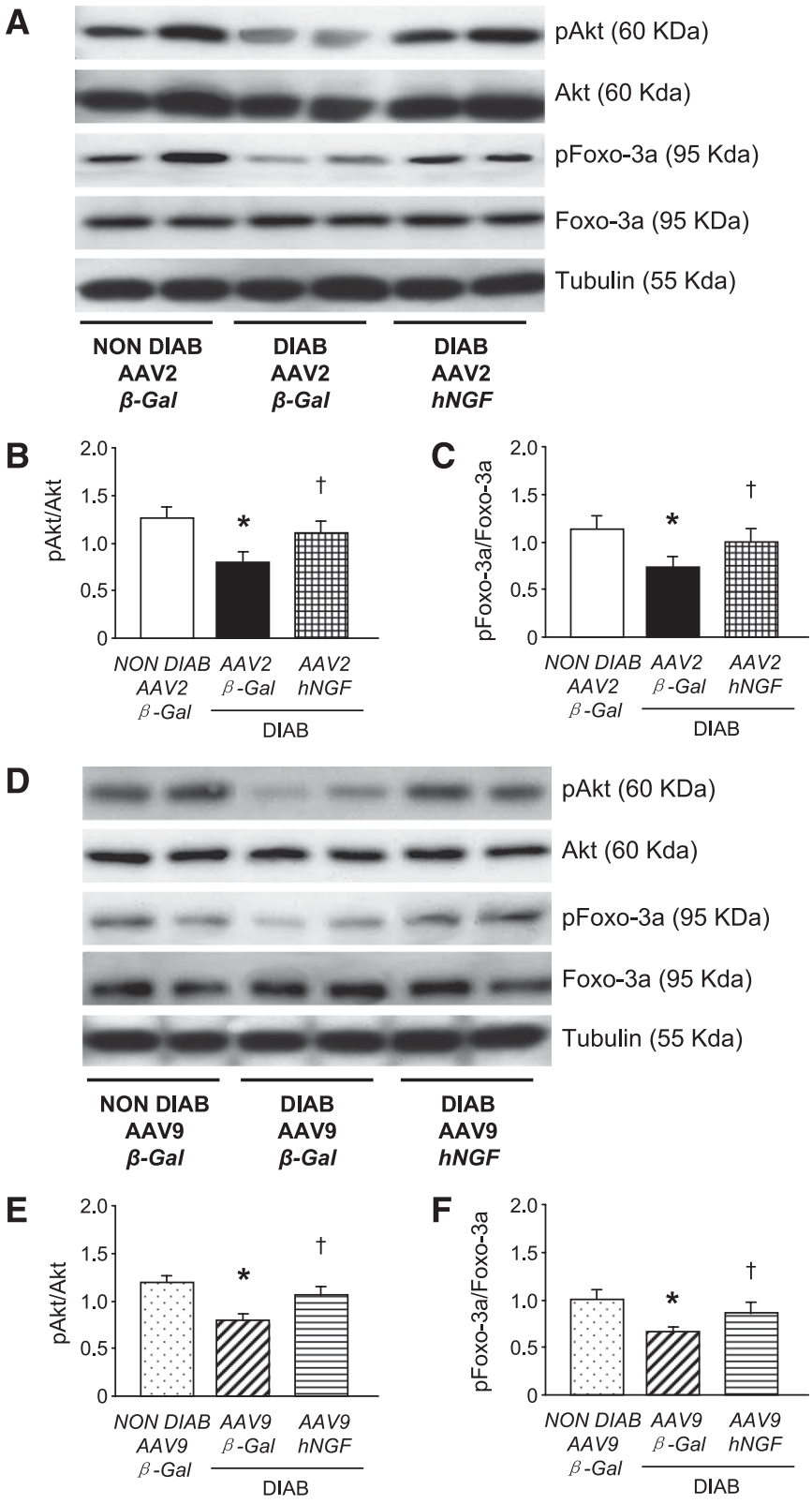

FIG. 5. Effects of *NGF* gene therapy on the Akt/Foxo3a pathway in the diabetic heart. *A*: Representative Western blot bands showing the impact of 12 weeks of diabetes (Diab) and AAV2-mediated *hNGF* gene transfer on the phosphorylation of Akt and Foxo3a. Bar graphs show the phosphorylation/activation of Akt (*B*) and phosphorylation/inactivation of Foxo3a (*C*) in AAV2-injected hearts. Representative Western blot bands (*D*) and normalization graphs (*E* and *F*) in AAV9-injected hearts. Data are expressed as means ± SEM. **P* < 0.05 vs. nondiabetes with AAV2–*β-Gal* or nondiabetes with AAV9–*β-Gal*; †*P* < 0.05 vs. diabetes with AAV2–*β-Gal* or diabetes with AAV9–*β-Gal* (*n* = 4 mice for each nondiabetes group and *n* = 5 mice for all other groups).

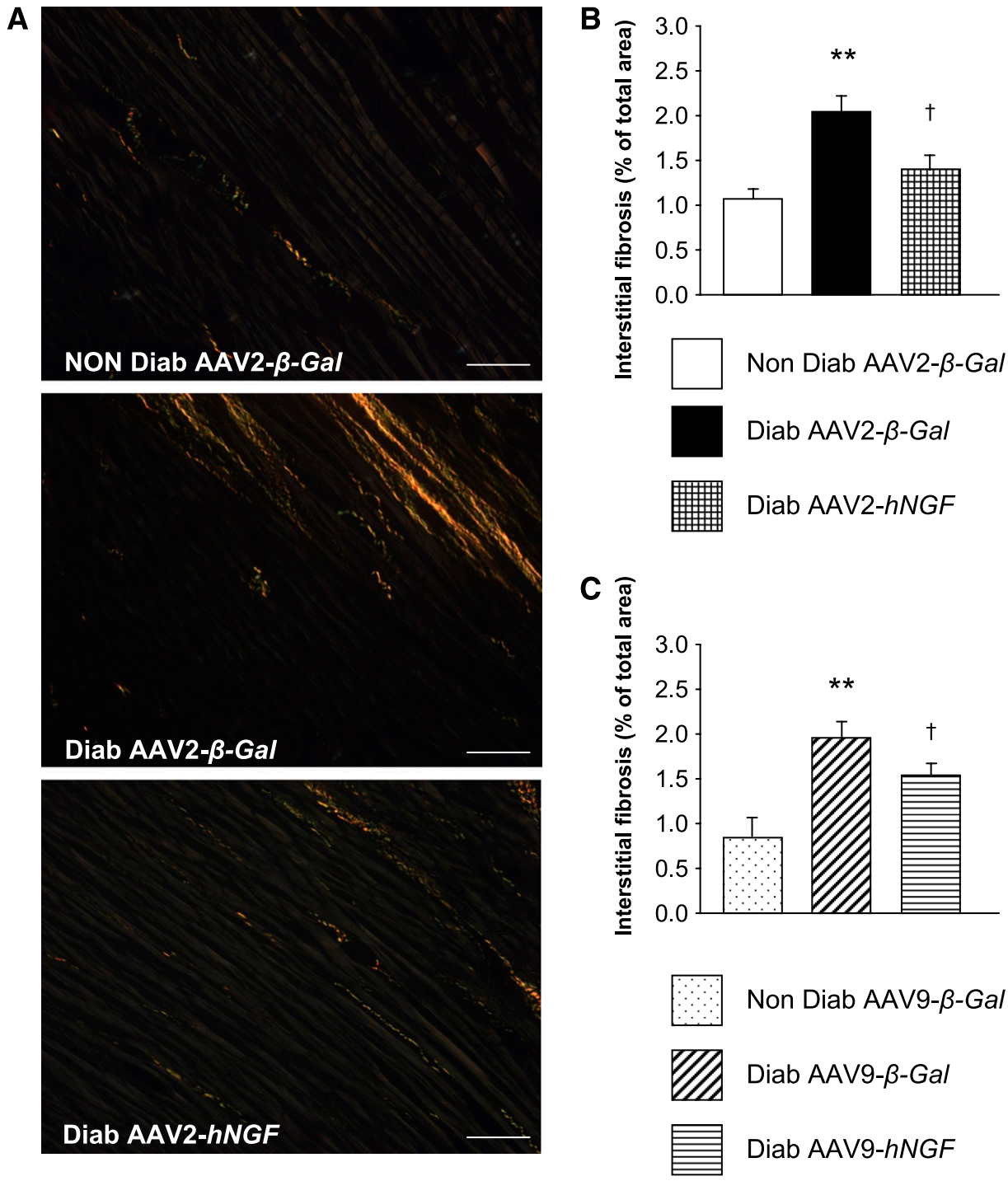

FIG. 6. Effect of *NGF* gene therapy on diabetes (Diab)-induced interstitial fibrosis. *A*: Representative microphotographs of left ventricle sections after Picrosirius Red staining. Collagen deposition is revealed in bright yellow via use of a polarized light (20× magnification). Bar graphs show the amount of interstitial fibrosis after either AAV2-mediated (*B*) or AAV9-mediated (*C*) gene therapy. Data are expressed as means ± SEM. **P < 0.01 vs. nondiabetes with AAV2–*β-Gal* or nondiabetes with AAV9–*β-Gal*; †P < 0.05 vs. diabetes with AAV2-*β-Gal* or diabetes with AAV9-*β-Gal* (n = 5 mice for each nondiabetes group and n = 6 mice for all other groups). (A high-quality digital representation of this figure is available in the online issue.)

diabetes induction). Indexes of left ventricle systolic dysfunction were evident at 8 weeks (reduced LVEF) and 12 weeks (reduced dP/dt_{max}, LVEF, and LVFS) after diabetes induction. Taken together, in line with previous reports these results support the presence of diabetes-induced early diastolic dysfunction followed by systolic dysfunction (30,36). Moreover, the diabetic heart is also characterized by structural changes and, in particular, by increased ventricular dilatation. Notably, echocardiography revealed significant increase in LVID as well as left ventricle chamber volume dilatation in *β-Gal*–injected diabetic hearts. Importantly, NGF overexpression in the diabetic heart prevented left ventricle diastolic and systolic dysfunction and reduced left ventricle chamber dimensions. These results suggest that lack of NGF is detrimental for cardiac performances in the diabetic heart at both earlier

and later stages of cardiomyopahty. On the other hand, *NGF* gene transfer appears utilitarian for improving cardiac function in diabetes. Diabetes is often characterized by cardiac autonomic neuropathy that results in sympathetic nerve damage and consequent alteration of circulating catecholamine levels and heart rate (38). Given that NGF regulates cardiac sympathetic innervation (9), it is possible that NGF overexpression could prevent nerve damage in the diabetic heart. In line with this, heart rate was higher in diabetic mice treated with hNGF. We did not evaluate the effects of NGF overexpression on cardiac innervations or plasma catecholamines, which represents a limitation of our study. Microvascular rarefaction is another common hallmark of the diabetic heart. Diabetic myocardial microangiopathy has been shown in both humans and rodents with streptozotocin-induced diabetes (39,40). Changes in the cardiac microvascular architecture are causally associated with increased apoptosis of endothelial cells, fibrosis deposition, and reduction of cardiac perfusion. Immunohistological analyses of heart sections at 12 weeks of diabetes confirmed a reduced number of capillaries and small-size arterioles and increased endothelial cell and cardiomyocyte apoptosis, confirming previous reports in diabetic patients and animals (41,42). The antiapoptotic and proangiogenic effects of NGF are well documented in several tissues and in different types of pathologies (4,5,7,43,44). The serine-threonine kinase Akt plays a crucial role in the prosurvival and proangiogenic effects of NGF (7,45,46). Phosphorylation/activation of Akt downstream of the NGF high-affinity receptor TrkA leads to the phosphorylation/inactivation of the Forkhead transcription factor Foxo3a, resulting in cardiomyocyte survival and angiogenesis (4,25). Moreover, Akt-Foxo signaling is altered in the diabetic heart (27). In agreement with our previous reports demonstrating the involvement of Akt/Foxo3a signaling in the prosurvival and proangiogenic effects of NGF (4,5), here we show that NGF overexpression increases Akt and Foxo3a phosphorylation in the diabetic heart, which may explain the cardioprotective effects. In the current study, we have found that AAV-mediated NGF cardiac overexpression preserves the vascular architecture of the diabetic myocardium. These significant effects of *NGF* gene transfer were also emphasized by increased myocardial perfusion in the presence of diabetes. Finally, another frequent feature of the diabetic heart is increased interstitial fibrosis, which results in increased left ventricle stiffness, thus compromising the ability of the heart to contract and relax efficiently (47,48). In line with this, histological analyses performed at 12 weeks of diabetes demonstrated accumulation of fibrotic content in the interstitial myocardium of *β-Gal*–injected diabetic mice, with a significant reduction after *NGF* gene transfer, indicating that NGF overexpression confers protection against cardiac fibrosis induced by diabetes.

At 12 weeks from gene transfer, similar cardiac hNGF mRNA expression was found in mice treated with AAV2 and AAV9. However, hNGF plasma levels were higher after AAV9. This is in line with the different tissue biodistribution observed in the two gene transfer approaches and suggests that the heart is not the only source of circulating hNGF after AAV9-*hNGF* injection. As the two gene transfer approaches resulted in comparable cardiac effects, it is possible that the amount of hNGF produced by AAV2-*hNGF* was sufficient to ensure optimal cardiac protection.

In conclusion, our results suggest that *NGF* gene transfer might have a tremendous therapeutic potential for the treatment of diabetic cardiomyopathy and encourage further translational efforts for the final benefit of diabetic patients. However, before this gene transfer approach can be tested in patients, additional preclinical studies need to be performed (including in larger animals) not only to verify the efficiency and the safety of AAV-mediated NGF overexpression in the setting of type 1 diabetes but also to find the most efficient AAV serotype, as well as the optimal dose and delivery route to be used. Moreover, since NGF is secreted and TrkA is present in several cell types, a better understanding of *NGF* gene transfer impact on noncardiac tissues and organs needs to be developed. Moreover, potential side effects common to all other proangiogenic and prosurvival factors (like tumor and ocular angiogenesis and inflammatory angiogenesis of joints) should also be considered. Finally, it seems important to preclinically evaluate the result of *NGF* gene transfer in association with insulin and other therapeutic treatments commonly used in diabetic patients.

ACKNOWLEDGMENTS

This study was funded by a European Programme in Type 1 Diabetes research grant from the European Foundation for the Study of Diabetes together with the Juvenile Diabetes Research Foundation and the Novo Nordisk (to C.E.). It was also funded by the British Heart Foundation senior research fellowship grant (to C.E.). I.F. was recipient of a bursary from the Sardinian regional government ("Master and Back" scheme). No other potential conflicts of interest relevant to this study were reported.

M.M. researched data and wrote the manuscript. B.D., A.C., and I.F. researched data. L.Z. prepared AAV vectors and reviewed and edited the manuscript. M.G. reviewed and edited the manuscript. C.E. ideated the study, obtained the funds for the research, and wrote the manuscript.

Parts of this study were presented in abstract form at the American Heart Association (AHA) Scientific Sessions, Orlando, Florida, 14–18 November 2009; at the British Microvascular Society Meeting, Exeter, U.K., 19–20 April 2010; and at the AHA Scientific Sessions 2010, Chicago, Illinois, 13–17 November 2010.

Drs. Rajesh Katare and Graciela-Sala Newby (both from University of Bristol) helped with measuring E-to-A ratio and with NGF vector preparation, respectively.

REFERENCES

1. Litwin SE, Raya TE, Anderson PG, Daugherty S, Goldman S. Abnormal cardiac function in the streptozotocin-diabetic rat. Changes in active and passive properties of the left ventricle. J Clin Invest 1990;86:481–488
2. Moir S, Hanekom L, Fang ZY, et al. Relationship between myocardial perfusion and dysfunction in diabetic cardiomyopathy: a study of quantitative contrast echocardiography and strain rate imaging. Heart 2006;92:1414–1419
3. Sabbah HN, Sharov VG, Lesch M, Goldstein S. Progression of heart failure: a role for interstitial fibrosis. Mol Cell Biochem 1995;147:29–34
4. Caporali A, Sala-Newby GB, Meloni M, et al. Identification of the prosurvival activity of nerve growth factor on cardiac myocytes. Cell Death Differ 2008;15:299–311
5. Meloni M, Caporali A, Graiani G, et al. Nerve growth factor promotes cardiac repair following myocardial infarction. Circ Res 2010;106:1275–1284
6. Cantarella G, Lempereur L, Presta M, et al. Nerve growth factor-endothelial cell interaction leads to angiogenesis in vitro and in vivo. FASEB J 2002;16:1307–1309
7. Emanueli C, Salis MB, Pinna A, Graiani G, Manni L, Madeddu P. Nerve growth factor promotes angiogenesis and arteriogenesis in ischemic hindlimbs. Circulation 2002;106:2257–2262

8. Hellweg R, Hartung HD. Endogenous levels of nerve growth factor (NGF) are altered in experimental diabetes mellitus: a possible role for NGF in the pathogenesis of diabetic neuropathy. J Neurosci Res 1990;26:258–267
9. Ieda M, Kanazawa H, Ieda Y, et al. Nerve growth factor is critical for cardiac sensory innervation and rescues neuropathy in diabetic hearts. Circulation 2006;114:2351–2363
10. Schmid H, Forman LA, Cao X, Sherman PS, Stevens MJ. Heterogeneous cardiac sympathetic denervation and decreased myocardial nerve growth factor in streptozotocin-induced diabetic rats: implications for cardiac sympathetic dysinnervation complicating diabetes. Diabetes 1999;48:603–608
11. Kaye DM, Vaddadi G, Gruskin SL, Du XJ, Esler MD. Reduced myocardial nerve growth factor expression in human and experimental heart failure. Circ Res 2000;86:E80–E84
12. Zincarelli C, Soltys S, Rengo G, Rabinowitz JE. Analysis of AAV serotypes 1-9 mediated gene expression and tropism in mice after systemic injection. Mol Ther 2008;16:1073–1080
13. Gao G, Vandenberghe LH, Wilson JM. New recombinant serotypes of AAV vectors. Curr Gene Ther 2005;5:285–297
14. Nathwani AC, Davidoff A, Hanawa H, Zhou JF, Vanin EF, Nienhuis AW. Factors influencing in vivo transduction by recombinant adeno-associated viral vectors expressing the human factor IX cDNA. Blood 2001;97:1258–1265
15. Pacak CA, Mah CS, Thattaliyath BD, et al. Recombinant adeno-associated virus serotype 9 leads to preferential cardiac transduction in vivo. Circ Res 2006;99:e3–e9
16. Ferrarini M, Arsic N, Recchia FA, et al. Adeno-associated virus-mediated transduction of VEGF165 improves cardiac tissue viability and functional recovery after permanent coronary occlusion in conscious dogs. Circ Res 2006;98:954–961
17. Arsic N, Zacchigna S, Zentilin L, et al. Vascular endothelial growth factor stimulates skeletal muscle regeneration in vivo. Mol Ther 2004;10:844–854
18. Grimm D, Kern A, Rittner K, Kleinschmidt JA. Novel tools for production and purification of recombinant adenoassociated virus vectors. Hum Gene Ther 1998;9:2745–2760
19. Inagaki K, Fuess S, Storm TA, et al. Robust systemic transduction with AAV9 vectors in mice: efficient global cardiac gene transfer superior to that of AAV8. Mol Ther 2006;14:45–53
20. Rabinowitz JE, Rolling F, Li C, et al. Cross-packaging of a single adeno-associated virus (AAV) type 2 vector genome into multiple AAV serotypes enables transduction with broad specificity. J Virol 2002;76:791–801
21. Emanueli C, Salis MB, Pinna A, et al. Prevention of diabetes-induced microangiopathy by human tissue kallikrein gene transfer. Circulation 2002; 106:993–999
22. Katare R, Caporali A, Zentilin L, et al. Intravenous gene therapy with PIM-1 via a cardiotropic viral vector halts the progression of diabetic cardiomyopathy through promotion of prosurvival signaling. Circ Res 2011;108:1238–1251
23. Yoon YS, Uchida S, Masuo O, et al. Progressive attenuation of myocardial vascular endothelial growth factor expression is a seminal event in diabetic cardiomyopathy: restoration of microvascular homeostasis and recovery of cardiac function in diabetic cardiomyopathy after replenishment of local vascular endothelial growth factor. Circulation 2005;111:2073–2085
24. Chowdhry MF, Vohra HA, Galinanes M. Diabetes increases apoptosis and necrosis in both ischemic and nonischemic human myocardium: role of caspases and poly–adenosine diphosphate–ribose polymerase. J Thorac Cardiovasc Surg 2007;134:124–131
25. Potente M, Urbich C, Sasaki K, et al. Involvement of Foxo transcription factors in angiogenesis and postnatal neovascularization. J Clin Invest 2005;115:2382–2392
26. Skurk C, Izumiya Y, Maatz H, et al. The FOXO3a transcription factor regulates cardiac myocyte size downstream of AKT signaling. J Biol Chem 2005;280:20814–20823
27. Lekli I, Mukherjee S, Ray D, et al. Functional recovery of diabetic mouse hearts by glutaredoxin-1 gene therapy: role of Akt-FoxO-signaling network. Gene Ther 2010;17:478–485
28. Stamler J, Vaccaro O, Neaton JD, Wentworth D. Diabetes, other risk factors, and 12-yr cardiovascular mortality for men screened in the Multiple Risk Factor Intervention Trial. Diabetes Care 1993;16:434–444
29. Van Linthout S, Spillmann F, Riad A, et al. Human apolipoprotein A-I gene transfer reduces the development of experimental diabetic cardiomyopathy. Circulation 2008;117:1563–1573
30. Katare RG, Caporali A, Oikawa A, Meloni M, Emanueli C, Madeddu P. Vitamin B1 analog benfotiamine prevents diabetes-induced diastolic dysfunction and heart failure through Akt/Pim-1-mediated survival pathway. Circ Heart Fail 2010;3:294–305
31. Bugger H, Abel ED. Rodent models of diabetic cardiomyopathy. Dis Model Mech 2009;2:454–466
32. Levi-Montalcini R. The nerve growth factor. Ann N Y Acad Sci 1964;118: 149–170
33. Hiltunen JO, Laurikainen A, Väkevä A, Meri S, Saarma M. Nerve growth factor and brain-derived neurotrophic factor mRNAs are regulated in distinct cell populations of rat heart after ischaemia and reperfusion. J Pathol 2001;194:247–253
34. Bartlett RJ, McCue JM. Adeno-associated virus based gene therapy in skeletal muscle. Methods Mol Biol 2000;133:127–156
35. Johnson JS, Samulski RJ. Enhancement of adeno-associated virus infection by mobilizing capsids into and out of the nucleolus. J Virol 2009;83: 2632–2644
36. Schannwell CM, Schneppenheim M, Perings S, Plehn G, Strauer BE. Left ventricular diastolic dysfunction as an early manifestation of diabetic cardiomyopathy. Cardiology 2002;98:33–39
37. Palmieri V, Capaldo B, Russo C, et al. Uncomplicated type 1 diabetes and preclinical left ventricular myocardial dysfunction: insights from echocardiography and exercise cardiac performance evaluation. Diabetes Res Clin Pract 2008;79:262–268
38. Fang ZY, Prins JB, Marwick TH. Diabetic cardiomyopathy: evidence, mechanisms, and therapeutic implications. Endocr Rev 2004;25:543–567
39. Fischer VW, Barner HB, Larose LS. Pathomorphologic aspects of muscular tissue in diabetes mellitus. Hum Pathol 1984;15:1127–1136
40. Cameron DP, Amherdt M, Leuenberger P, Orci L, Stauffacher W. Microvascular alterations in chronically streptozotocin-diabetic rats. Adv Metab Disord 1973;2(Suppl 2): 257–269
41. Frustaci A, Kajstura J, Chimenti C, et al. Myocardial cell death in human diabetes. Circ Res 2000;87:1123–1132
42. Cai L, Li W, Wang G, Guo L, Jiang Y, Kang YJ. Hyperglycemia-induced apoptosis in mouse myocardium: mitochondrial cytochrome C-mediated caspase-3 activation pathway. Diabetes 2002;51:1938–1948
43. Salis MB, Graiani G, Desortes E, Caldwell RB, Madeddu P, Emanueli C. Nerve growth factor supplementation reverses the impairment, induced by type 1 diabetes, of hindlimb post-ischaemic recovery in mice. Diabetologia 2004;47:1055–1063
44. Graiani G, Emanueli C, Desortes E, et al. Nerve growth factor promotes reparative angiogenesis and inhibits endothelial apoptosis in cutaneous wounds of Type 1 diabetic mice. Diabetologia 2004;47:1047–1054
45. Holgado-Madruga M, Moscatello DK, Emlet DR, Dieterich R, Wong AJ. Grb2-associated binder-1 mediates phosphatidylinositol 3-kinase activation and the promotion of cell survival by nerve growth factor. Proc Natl Acad Sci USA 1997;94:12419–12424
46. Park MJ, Kwak HJ, Lee HC, et al. Nerve growth factor induces endothelial cell invasion and cord formation by promoting matrix metalloproteinase-2 expression through the phosphatidylinositol 3-kinase/Akt signaling pathway and AP-2 transcription factor. J Biol Chem 2007;282: 30485–30496
47. Shimizu M, Umeda K, Sugihara N, et al. Collagen remodelling in myocardia of patients with diabetes. J Clin Pathol 1993;46:32–36
48. Devereux RB, Roman MJ, Paranicas M, et al. Impact of diabetes on cardiac structure and function: the strong heart study. Circulation 2000;101:2271–2276